



Original Article

Promotion of skin wound healing using hypoimmunogenic epidermal cell sheets

Hongqing Zhao ^{a, b}, Jiachen Sun ^b, Yating Wu ^b, Junbo Zhang ^{b, **}, Chuan'an Shen ^{c, *}^a Nanbu County People's Hospital, Nanchong City, Sichuan Province, 637300, China^b Jinzhou Medical University, No.82 Songpo Road, Guta District, Jinzhou 121001, Liaoning Province, China^c Department of Burn Surgery, Fourth Medical Center, PLA General Hospital, No 51 Fucheng Road, Haidian District, Beijing 100089, China

ARTICLE INFO

Article history:

Received 15 March 2023

Received in revised form

28 June 2023

Accepted 10 July 2023

Keywords:

Epidermal cell sheet

Indoleamine 2,3-dioxygenase

Skin

Wound healing

Allogenic skin substitute

ABSTRACT

Objective: The physiological process of wound healing is dynamic, continuous, and intricate. Nowadays, full-thickness burn wounds are treated by autologous skin transplantation. Unfortunately, when substantial burns develop, there are fewer donor sites accessible, making it difficult to satisfy the requirement for large-scale skin transplants and increasing the risk of patient mortality. This study investigated the possibility of using a newly created hypoimmunogenic epidermal cell sheet to heal skin wounds.

Methods: Transfection with lentivirus was used to generate Keratinocytes (KCs) that overexpress Indoleamine 2,3-Dioxygenase (IDO). Western blotting and quantitative polymerase chain reaction were used to measure IDO levels. To evaluate the function of IDO⁺ keratinocytes, CCK-8 and Transwell assays were performed. In cell sheet induction media, KCs and Fibroblasts (FBs) were cultured to yield epidermal cell sheets. The full-thickness skin excisions of BALB/c mice were transplanted with epidermal cell sheets. To assess the tumorigenicity of IDO⁺ keratinocytes, BALB/c nude mouse xenograft models were also used. CD3 and CD31 immunofluorescence labeling of wound tissue on day 12 to identify T lymphocyte infiltration and capillary development. ELISA measurement of IL-1 and TNF- α concentrations.

Results: IDO⁺ keratinocytes dramatically enhanced the expression levels of IDO mRNA and protein, as well as the amount of kynurenine in the conditioned media of IDO⁺ keratinocytes, compared to the Control and NC groups. CD8⁺ T cell apoptosis was considerably greater in the IDO group than in the Control and NC groups. Nevertheless, the proliferation and migratory capabilities of IDO⁺ keratinocytes were not substantially different from those of the Control and NC groups. In vitro cultivation of the hypoimmunogenic epidermal cell sheet was effective. In vivo transplantation experiments demonstrated that IDO⁺ epidermal cell sheets can effectively promote wound healing without tumorigenicity, and IDO⁺ epidermal cell sheets may promote wound healing by decreasing the expression levels of inflammatory factors (TNF and IL-1) in wound tissue, decreasing CD3⁺ T lymphocytes, and increasing infiltration and new capillaries in wound tissue.

Conclusion: In this study, we successfully constructed the hypoimmunogenic epidermal cell sheet and demonstrated that the hypoimmunogenic epidermal cell sheet could accelerate wound healing.

© 2023, The Japanese Society for Regenerative Medicine. Production and hosting by Elsevier B.V. This is an open access article under the CC BY-NC-ND license (<http://creativecommons.org/licenses/by-nc-nd/4.0/>).

1. Introduction

Wound healing is a dynamic, progressive, and complicated physiological process involving several cellular processes, including proliferation, adhesion, chemotaxis, and apoptosis [1]. The

epidermis, dermis, and accessory organs such as hair follicles, sweat glands, and sebaceous glands are destroyed by a full-thickness skin defect or severe burn. The two most critical cells involved in wound healing [2] are skin fibroblasts (FBs) and keratinocytes (KCs). At present, the treatment of full-thickness burn wounds relies on autologous skin transplantation. Nowadays, full-thickness burn wounds are treated by autologous skin transplantation [3]. Recently, high-density cell sheet structures containing solely cells and their secreted extracellular matrix have been manufactured using cell sheet technology. These cultivated sheets may be transplanted into specific host tissues without the

* Corresponding author.

** Corresponding author.

E-mail addresses: zhangjunbo_surgery@126.com (J. Zhang), shenchuanan@163.com (C. Shen).

Peer review under responsibility of the Japanese Society for Regenerative Medicine.

need for biodegradable scaffolds or sutures. Also produced are cell sheets, including two or more types of cell sources [4,5]. Nevertheless, when substantial burns occur, donor sites are restricted, making it difficult to fulfill the need for large-scale skin (or allogenic skin replacement) grafts, thereby increasing the risk of patient mortality [6]. In spite of the efficacy of skin autotransplantation, the high immunogenicity of the skin limits the use of allografts, and systemic immunosuppression is often ineffective for isolated skin grafts [7].

Indoleamine 2,3 dioxygenase (IDO) is a potent immunomodulatory enzyme with allo- and auto-immune suppression and tolerance induction characteristics in several physiologic and pathological contexts [8,9]. IDO, for instance, is capable of suppressing the maternal T lymphocyte immune response against semi-allogeneic fetal tissues during pregnancy via multiple mechanisms, including the production of immune-inhibitory metabolites [Kynurenine (Kyn) and Kynurenic Acid (KynA)] and the generation of a tryptophan-deficient environment [10]. Furthermore, it has been shown that IDO-expressing dendritic cells (DCs) neither sequester nor fail to deliver antigens. Instead of undergoing clonal proliferation and developing into effector cells, activated T cells experience apoptosis, become anergic, or transition into T regulatory cells [11,12] due to IDO activity in DCs. Hence, it has been hypothesized that the immunoregulatory function of IDO may be used therapeutically to suppress alloreactive immune responses. Research has shown that IDO overexpression reduces the rejection of islet allografts in mice [13–15]. This indicates that IDO expression may protect solid organ allotransplantation without the need for systemic immunosuppressive drugs.

In this work, we successfully created hypoimmunogenic cell sheets from IDO-overexpressed keratinocytes and implanted them into mouse wounds. Hypoimmunogenic cell sheets were shown to be feasible and to have an immune-protective effect.

2. Materials and methods

2.1. Cell isolation and culture

Human skin samples were collected from the Fourth Medical Center of PLA General Hospital with ethical approval and informed consent. The FBs and KCs were extracted as previously described [16,17]. The acquired skin tissue was cleansed with PBS (500 ml, Cat #G420, ServiceBio) three times before the subcutaneous tissue and adipose tissue were removed, and the skin tissue was clipped to make it regular. Subsequently, the skin tissue was put into the Dispase II enzyme (2.5 mg/ml, Cat #D4693-1G, Sigma) for digestion overnight at 4 °C, and the epidermis and dermis were separated the following day. The epidermis was digested with trypsin (0.25%, Cat # 25200072, Gibco) for about 30 min at 37 °C until the tissue was entirely digested. The dermis was digested with Type IV collagenase (0.25%, Cat # 17104019, Gibco). The cell suspension was filtered using a 70 µm cell sieve. KCs were cultured in serum-free defined Epilife (Cat # Mepicf500, Gibco) with 1% HKGS (Cat #S0015, Gibco). FBs were cultured in DMEM (Cat # SH30022.01, Hyclone) that contains 10% fetal bovine serum (Cat # 10099141C, Gibco). The HepG2 cells were donated by Peking University People's Hospital and were also cultured in DMEM (Cat # SH30022.01, Hyclone) that contains 10% fetal bovine serum (Cat # 10099141C, Gibco). All the cells were cultured without antibiotics in the incubators (5% CO₂, 37 °C). The medium was changed every day.

2.2. RNA extraction and qPCR analysis

RNA extraction and qPCR assays were performed as previously described [18]. The total RNA was extracted from the cells with

Trizol reagent (Cat # 15596026, Thermo Fisher) and reverse transcribed into cDNA with the FastKing gDNA Dispelling RT SuperMix (Cat # KR118, TianGen, China), as recommended by the manufacturer. qPCR was conducted, and SYBR Green Supermix (Cat #1708882AP, Bio-Rad, USA) was used for the relative quantification of the genes. The CT value of each well was detected and recorded, and $2^{-\Delta\Delta CT}$ was used to normalize the gene expression of the sample to the expression of GAPDH. The following primer pairs were used: IDO– Forward primer: AGTCATCGGTCAGACACCCTT; Reverse primer: GTGCAGCGTTATCTCCAACAG; COL4A1- Forward primer: GGACTACCTGGAACAAAAGGG; Reverse primer: GCCAAGTATCTCACCTGGATCA; LAMA1- Forward primer: GTCAGCGACTCAGAGTGTG; Reverse primer: CTGGGTGAAAGATCGTCAGC.

2.3. Western blot assays

Western blot analysis was performed as previously described [19]. The total proteins were isolated using RIPA buffer (Cat # 89901, Thermo Fisher) containing protease (Cat # 36978, Thermo Fisher) and phosphatase inhibitors (Cat # A32957, Thermo Fisher). The BCA Protein Assay Kit (Cat # 23225, Thermo Fisher Scientific, Waltham, MA, USA) was used to determine the protein concentration. After blocking with 10% nonfat milk, the membranes were probed overnight at 4 °C with gentle shaking with primary antibodies including rabbit anti-IDO (Cat # 86630S, 1:1000, CST), rabbit anti-COL4A1 (Cat # 50273S, 1:1000, CST), rabbit anti-LAMA1 (Cat # 37710S, 1:1000, CST) and GAPDH (Cat #5174S, 1:2000, rabbit monoclonal, CST). The protein bands were detected using ChemiDoc XRS chemiluminescence imaging equipment (Bio-Rad).

2.4. CCK8 assays

The cells were seeded into a 96-well plate and left to grow while adhering to the surface for 8 h. 10 µl of CCK8 reagent (Cat # HY-K0301, MCE) was applied to each well, and then the cells were cultured at 37 °C for 4 h before a multifunctional microplate reader (Biotek Synergy2, USA) was utilized to measure the absorbance at 6, 12 and 24 h at 450 nm wavelength.

2.5. Transwell assays

The cells were planted onto the transwell plates. The mixed cell culture medium (DMEM high glucose medium + 10% fetal bovine serum + 1% EGF) was introduced to the bottom compartment. Cellular migration was examined at 48 h after seeding [20].

2.6. Ido gene lentivirus transfection

The IDO lentivirus vector (pLVXAcGFP1-puro) was purchased from GeneChem (Shanghai, China). Following the manufacturer's instructions, keratinocyte cells (3×10^5 cells/well) were planted in a 6-well plate. When the cells were fused to 50–60%, multiplicity of infection (MOI = 50) was used to transfect the cells, 80 µl of lentivirus stock solution and 40 µl of transfection reagent (HiTransG P) were added to 100 µl of DMEM, and the culture plate was gently shaken so that the venom could cover every cell. It was then incubated overnight (12 h) in a carbon dioxide incubator at 37 °C and 5% CO₂. The next day, the culture medium containing the virus was pulled out and the cells were cultured with fresh complete culture medium and 2 µg/ml puromycin. The fresh and complete medium was replaced daily until a stable IDO⁺ keratinocyte cell was constructed.

2.7. Kynurenine assay

Measuring the quantities of the tryptophan-degraded product L-kynurenine in the conditioned media obtained from IDO-transfected cells and control vector-transfected cells allowed for the evaluation of IDO's biological activity. Using a previously described approach [21], the quantity of L-kynurenine was quantified. Briefly, the proteins in the conditioned medium were precipitated with trichloroacetic acid, and following centrifugation, 0.5 ml of the supernatant was incubated for 10 min at room temperature with an equivalent amount of Ehrlich's reagent. Within 2 h, the absorbance of the resulting solution was measured at 490 nm using a spectrophotometer. Kynurenine concentrations in the conditioned medium were determined using a standard curve with a known kynurenine concentration (0–100 mM).

2.8. Hematoxylin and eosin staining

The freshly removed tissue from the Control, NC, and IDO groups, as well as the tumor tissue from the HepG2 group, was fixed in 4% paraformaldehyde for 24 h, dehydrated, paraffin-embedded, sectioned, and stained with Hematoxylin and eosin according to the protocol described previously [22]. The acquired paraffin slices were deparaffinized, stained with hematoxylin-eosin (Cat #C0105 M, Beyotime), dried, and then mounted. Using an optical microscope, histological changes were found in the tissue sections (Nikon DS-U3).

2.9. Immunofluorescence and immunohistochemistry

The tissues were fixed with 4% paraformaldehyde for 30 min and then permeabilized with 0.25% Triton X-100 (Catalog #X100, Sigma) for 10 min prior to immunofluorescence labeling. To inhibit non-specific epitope binding, tissues were incubated with phosphate buffer containing 1% bovine serum albumin (Cat# A1933, Merck) and 0.1% Tween-20 (Cat# P7949, Sigma) for 1 h, followed by overnight incubation at 4 °C with the following primary antibodies: mouse anti-CD31 (Cat #3528S, 1:100, CST) and rabbit anti-CD3 (Cat #26582, CST). The nuclei were then stained with DAPI (Cat #d1306, Thermo Fisher).

Immunohistochemistry was performed using the primary antibodies mouse anti-CK5 (Cat#66727-1-Ig, 1:200, Proteintech) and rabbit anti-IDO (Cat# 86630S, 1:1000, CST). Subsequently, tissue sections were deparaffinized and treated with antibodies overnight at 4 °C. They were then rinsed with PBS followed by staining with donkey anti-mouse or anti-rabbit IgG antibodies. Hematoxylin was employed to counterstain the sections.

2.10. Co-culture of keratinocytes with CD8⁺ T cells and apoptosis detection

Control, NC, and IDO cells were planted at a density of 2×10^5 cells per well in 6-well plates for 24 h. Peking University Peoples' Hospital contributed the CD8⁺ T cells. 1×10^6 CD8⁺ T cells were added to each well for co-culture, and enriched RPMI and DMEM were mixed 50:50 as the culture medium.

Following 6 h of incubation, 2 ml of complete DMEM media was reintroduced and the cells were cultured for an additional 24 h. Using flow cytometry and the cell cycle detection kit in line with the manufacturer's procedure, the cell cycle status was determined. Using flow cytometry and the FITC-Annexin V/PI apoptosis detection kit [23], the apoptosis of cells was analyzed.

2.11. Elisa assays

Collect mouse wound tissue, wash it with PBS, place the tissue block in a glass homogenizer, add 10 ml of pre-chilled PBS, and grind it completely at 4 °C. The resultant homogenate may be further processed by ultrasonic crushing, and the produced homogenate can be utilized immediately. The slurry was centrifuged for 5 min at 5000g, and the supernatant was collected. The TNF- α and IL-1 ELISA kits were purchased from Krishgen Biosystems, USA. The wells were then sealed with adhesive tape and incubated at 37°C for 90 min. Except for the blank wells, each well received 100 μ l of biotinylated antibody solution. The wells were then sealed with adhesive tape and kept at 37 °C for 60 min. The enzyme solution was made in advance for 30 min and stored at room temperature out of direct sunlight. 100 μ l of enzyme solutions were added to each well after washing. Wells were sealed with adhesive tape and kept at 37 °C for 30 min. Except for the blank wells, chromogenic substrate was added to each well after washing. The plates were then incubated at 37 °C for 10–15 min in the dark. Within 10 min, the stop solution was added to each well and well mixed. The OD450 value was then measured [24].

2.12. Preparation of in vitro-engineered epidermal cell sheets

Constructing Epidermal Cell Sheets Medium: DMEM high-glucose medium: F12 medium at a ratio of 3:1 and adding 10% fetal bovine serum by volume to create the baseline medium, followed by the addition of 1% antibiotics and 1% HKGS solution. For every 100 ml of culture medium, add 0.5 ml of adenine solution with a concentration of 4.8 mg/ml, 13 μ l of thyroxine solution with a concentration of 1 mg/ml, and 85 μ l of cholera toxin solution with a concentration of 0.5 mg/ml. Shake after combining. Combine well and keep aside.

The source of the cell-sheet scaffolds was fibroblasts. When fibroblasts reach 70%–80% confluence, add 2.5 ml of a 4 μ g/ml Mitomycin C solution, incubate at 37 °C for 2 h, then wash with PBS for 3 min. Repeat 5 times and closely regulate the experiment's duration. The keratinocytes were seeded into the cell sheet scaffolds, the cells were resuspended with the prepared epidermal cell sheet media, and they were inoculated onto a 6-well plate containing 5×10^6 fibroblasts by adding 2 ml of solution. After 14–17 days, the cell sheet will have attained an appropriate thickness if the medium is changed daily. After 14–17 days, the cell sheets were produced and transplant-ready.

2.13. Animals and transplantation

The animal experiment was conducted in accordance with procedures authorized by the Fourth Medical Center's Ethics Committee and in accordance with the standards of the Institutional Animal Care and Use Committee. Male BALB/c mice (8 weeks old) were obtained from SPF Biotechnology (Beijing, China) and randomized into four groups of 15 mice each. As detailed by Wu et al. [25], a 5mm \times 5 mm full-thickness skin defect was generated on the dorsum of mice. Completely cover the wound with the cell sheets, then secure them with a 3 M anti-contraction ring. Every two days, replace old cell sheets with fresh ones. The wounds were photographed on the 4th, 8th, and 12th days after injection. Wound healing ratio = (original wound area - residual wound area)/100%.

2.14. Tumorigenicity assay

BALB/c nude mice (male, 8 weeks old) were obtained from SPF Biotechnology (Beijing, China) and randomly divided into three groups of six mice each: NC, IDO, and HepG2. The NC, IDO, and

HepG2 cells were suspended in PBS at a concentration of 5×10^6 cells per 100 μl . 100 μl of the prepared cell suspension was then injected into the subcutaneous tissue of each nude mouse in each of the three groups. The mice were killed forty days after inoculation. The tumor's size was determined, and it was removed for histological analysis [26].

2.15. Statistical analysis

All data were expressed as the mean \pm standard deviation (SD). The one-way analysis of variance (ANOVA) was performed for the analysis between three or more groups, and the two-way ANOVA with Tukey's multiple comparisons test analysis was used to analyze the multivariate data. P values < 0.05 were considered statistically significant. Statistical analysis was performed with the program GraphPad Prism.

3. Results

3.1. Characteristics of keratinocytes overexpressing IDO

We identified the influence of IDO on the mRNA and protein expression of IDO in keratinocytes. We discovered that IDO treatment considerably increased the mRNA levels of IDO relative to untreated control cells and treated NC cells (Fig. 1a). Fig. 1b demonstrates that the protein levels of IDO in keratinocyte cells treated with IDO were significantly greater than those in the control and NC groups. Before any *in vivo* investigations were conducted, the rate of IDO activity was measured. The IDO activity in the medium that had been conditioned was then determined [27]. As demonstrated in Fig. 1c, the levels of kynurenine in the conditioned media of IDO-infected keratinocytes were considerably higher than those of Control or NC keratinocytes. There was no significant difference between Control, NC, and IDO⁺ keratinocyte proliferation rates at the 6th, 12th, and 24th hours of culture (Fig. 1d). 24 h after culture, there was no substantial variation in their migratory rate (Fig. 1e). Keratinocytes and CD8⁺ T cells were co-cultured for 24 h to see whether IDO had an immune-protective effect. The results demonstrated that the apoptosis rate of CD8⁺ T cells in the IDO group was considerably greater than in the control and NC groups. These offer the biological foundation for the development of hypoimmune epidermal cell sheets (Fig. 1f). Consequently, it was verified that the IDO gene increased IDO expression levels in keratinocytes *in vitro*. Compared to the control and NC groups, IDO⁺ keratinocytes exhibit comparable proliferative and migratory capabilities and efficient immune protection.

3.2. IDO⁺ keratinocytes were not tumorigenic

For potential therapeutic applications of hypoimmunogenic epidermal cell sheets in wound healing, their safety cannot be overlooked. To investigate the possibility of IDO + keratinocytes inducing subcutaneous carcinogenesis, a test was done on nude mice. On the 40th day after the injection of cells into each group, neither the NC nor IDO groups displayed any obvious evidence of carcinogenesis. In the HepG2 group, however, the growth of additional organisms at the injection site was seen. Extracted and weighed were the skin from the injection sites of the NC and IDO groups and the tumor tissue from the HepG2 group (Fig. 2a). HE staining of tumor tissue in the HepG2 group indicated a significant degree of neutrophil infiltration, a disorganized distribution of local cells, vacuolation of the cytoplasm, and enhanced atypia and irregular nuclei in the tumor cells, while the NC and IDO groups exhibited normal skin structure. (Fig. 2b). Immunostaining tumors *in vivo* with the CK5 antibody revealed that IDO⁺ keratinocytes are

not carcinogenic (Fig. 2c). Our results demonstrated that IDO⁺ keratinocytes cannot induce malignancy.

3.3. Characteristics of IDO⁺ keratinocyte sheets

Following 14–17 days of keratinocyte and fibroblast culture, transplantable epidermal cell sheets were effectively created (Fig. 3a). To confirm the expression of the IDO gene in epidermal cell sheets, we collected mRNA and protein from 17-day-cultured epidermal cell sheets for qPCR and Western blot analysis. In low-immunogenic epidermal cell sheets, the expression of IDO was considerably greater than in the control and NC groups (Fig. 3b and c). The epithelial layer of the cell sheet was composed of 2–4 layers of cuboidal nucleated epithelial cells interspersed with elongated cells, according to histological investigations. Inside the scaffold, fibroblasts constitute the subepithelial layer of the cell sheets (Fig. 3d). In the meanwhile, we conducted IDO immunohistochemistry labeling on the produced epidermal cell sheet, and the findings showed that 2–4 layers of epithelial cells with significant IDO expression remained in the IDO⁺ cell sheet (Fig. 3f). To validate the immunity of IDO⁺ epidermal cell sheets, after 17 days of growth we treated CD8⁺ T lymphocytes with the cell sheet culture medium and measured the apoptosis rate of CD8⁺ T lymphocytes. According to the data, the apoptosis rate of CD8⁺ T cells in the IDO cell sheet group was considerably higher than in the control and NC groups. To evaluate the engraftment rate of the cell sheets, we detected the expression of basement membrane proteins (COL4A1 and LAMA1) in the cell sheets, and the results showed that the cell sheets of all groups had high expression of COL4A1 and LAMA1 with no statistical difference. In other words, IDO genes do not affect the transplantation rate of cell sheets. The cell sheets have good histocompatibility and engraftment rates (Fig. 6). All of the foregoing data revealed that low-immunogenic cell sheets overexpressing IDO were effectively created.

3.4. Therapeutic effects of hypoimmunogenic epidermal cell sheets

To investigate the therapeutic advantages of hypoimmunogenic epidermal cell sheets on wound healing, full-thickness (5 mm) dorsal skin wounds were created on BALB/c mice (male, 8 weeks old), treated with control, NC, or IDO, and then examined on days 4, 8, and 12. On days 4 and 8, there was no statistically significant difference between the control, NC, and IDO groups (day 4: $50.40 \pm 2.02\%$, $51.80 \pm 0.67\%$, and $51.20 \pm 1.18\%$; day 8: $73.80 \pm 3.52\%$, $72.60 \pm 6.97\%$, and $74.20 \pm 4.52\%$, respectively). On day 12, the wounds treated with IDO healed faster than those in the control and NC groups (IDO: $96.8 \pm 0.67\%$, control: $90.20 \pm 3.32\%$ and NC: $88.40 \pm 2.52\%$), whereas the wound healing ratio in the control group did not significantly differ from that in the NC group (Fig. 4a).

At the same time, the Control, NC, and IDO groups observed abnormal skin structure (no complete epithelial structure) in the recovery of the Control and NC groups on the 12th day after injury, whereas the IDO group displayed a relatively complete skin structure closer to the physiological state, indicating that the wound healing effect of the IDO group was superior to that of the Control and NC groups (Fig. 4b). At 12 days post-injury, the IDO group's gene and protein expression levels were considerably greater than those of the Control and NC groups (Fig. 4c). In order to validate that IDO⁺ keratinocytes are intimately associated with wound healing, wounds were immunohistochemically stained on day 12 with a human-specific IDO antibody, and IDO⁺ keratinocytes were found in certain hair follicle-like structures in the IDO group (Fig. 4d). The degree of re-epithelialization of wound tissue was greater in the IDO group than in the control and NC groups. These findings

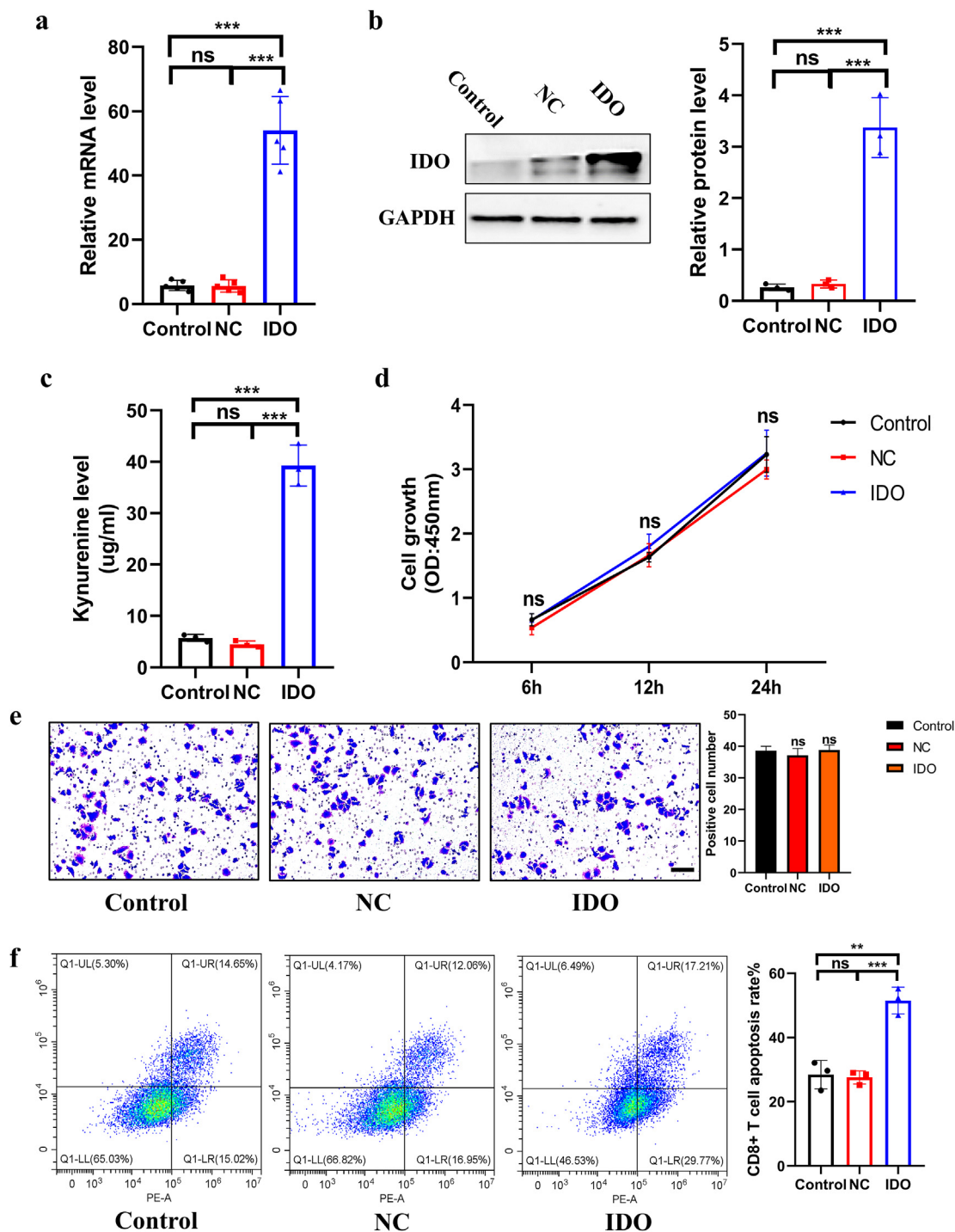


Fig. 1. Features of keratinocytes overexpressing IDO. **a.** Quantitative reverse transcription polymerase chain reaction was used to detect the gene expression of IDO. (***P < 0.001, n = 3). **b.** Expression of IDO protein was evaluated in the Control, NC and IDO group by Western blot analysis (***P < 0.001, n = 3). **c.** Kynurenine levels in IDO transfected keratinocytes conditioned medium. Conditioned medium was collected from the same number of infected and non-infected cells at 72 h post-transfection. Kynurenine levels were determined (***P < 0.001, n = 3). **d.** CCK8 assay showed the proliferative ability of Control, NC and IDO group (n = 3). **e.** Transwell test was used to analyze cell migration, and the number of positive cells was counted. (Scale bar, 10 μm n = 3). **f.** Analysis of apoptosis of CD8⁺ T lymphocytes by flow cytometry (***P < 0.001, n = 3).

revealed that the IDO group has greater wound healing capability and potential.

3.5. The potential role of IDO⁺ epidermal cell sheets in wound healing

There are contradictory data on the survival and immunological response of allografts of cultivated skin cells, particularly fibroblasts

and keratinocytes [28–30]. As with other cell types [31], however, xenogeneic fibroblasts and keratinocytes have been demonstrated to elicit a robust immunological response in the host [30,32,33]. Determine whether IDO has a function in preventing the immunological rejection of transplanted skin cells.

As shown in Fig. 5a and d, immunofluorescent staining of CD3⁺ T lymphocytes on the tissues 12 days after injury revealed that the number of CD3⁺ T lymphocyte infiltration in the IDO group was

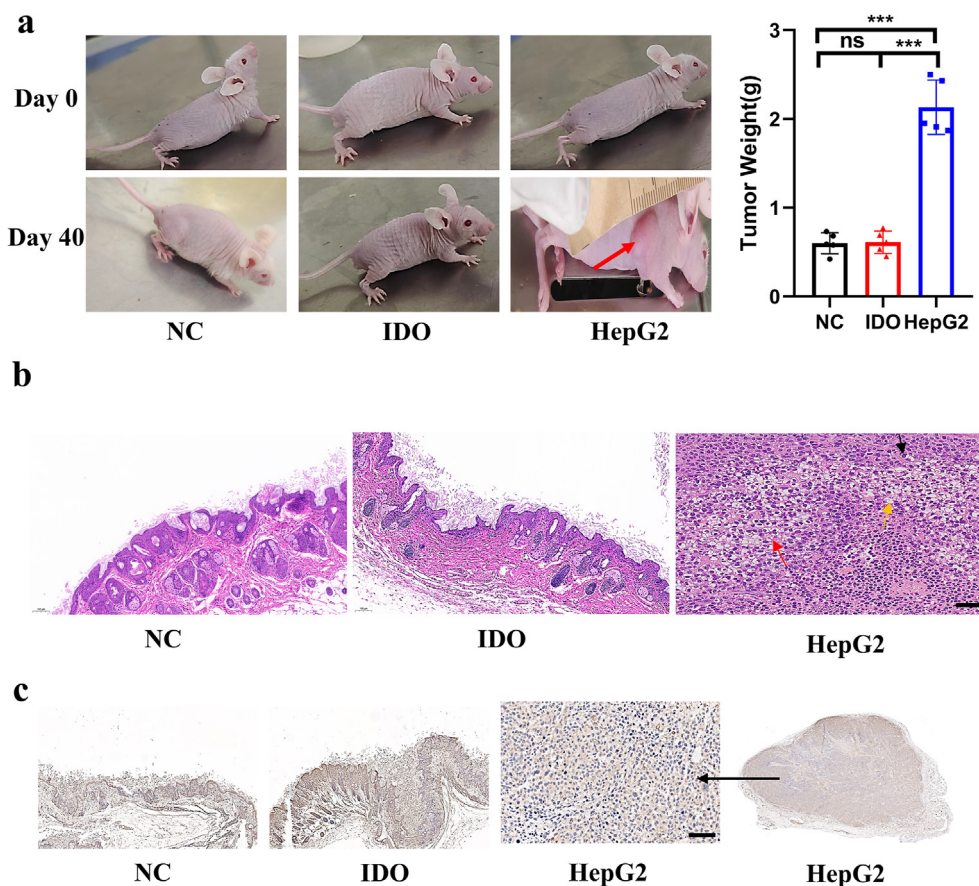


Fig. 2. Keratinocytes overexpressing IDO were not tumorigenic. **a.** The tumorigenicity test of Control, NC and IDO cells in nude mice (the area indicated by the red arrow on day 0 is the cell injection site, and the area marked by the red arrow on day 40 is subcutaneous tumor on day 40 after cell injection, $***P < 0.001$, $n = 5$) **b.** HE staining of tumors in the NC, IDO and HepG2 group. NC and IDO group showed normal skin tissue, while there was a large number of infiltrated neutrophils in the HepG2 group was observed, as shown by the yellow arrow; the local cells were loosely arranged, and the cytoplasm was vacuolated, as shown by the red arrow; a large number of tumor cells in the tissue increased atypia, and the nucleus was obviously irregular, as indicated by the black arrow (Scale bar, 100 μm , $n = 5$). **c.** Immunohistochemical staining revealed CK5-positive cells in tumor tissues in the NC, IDO and HepG2 groups (Scale bar, 100 μm , $n = 5$).

significantly lower than that in the Control group and the NC group, while there was no significant difference between the Control group and the NC group. There is evidence that the IDO⁺ epidermal cell sheets generated by genetically engineered xenogeneic keratinocytes inhibit T lymphocyte infiltration at the wound site.

Delayed revascularization is believed to be a cause of allograft and xenograft rejection [34]. To further examine the impact of IDO on neovascularization in vivo, we stained skin tissue slices with CD31 immunofluorescent labeling 12 days after damage. The findings demonstrated that the number of capillary-like capillaries in the wounds of IDO + epidermal cell sheets was substantially greater than that of the Control and NC groups (Fig. 5b and c). ELISA was utilized to measure the expression levels of IL-1 and TNF- α in the supernatant of homogenized skin tissue 12 days after injury. The findings demonstrated that the levels of TNF- α and IL-1 in the supernatant of IDO tissue were considerably lower than those of the Control group and the NC group, although there was no significant difference between the Control group and the NC group (Fig. 5e). The aforementioned findings suggested that IDO⁺ epidermal cell sheets promoted wound healing by dramatically decreasing wound CD3⁺ T lymphocyte infiltration, lowering wound inflammation, and promoting wound capillary-like tissue development.

4. Discussion

In this study, we revealed that the proliferation and migratory abilities of IDO + keratinocytes and primitive keratinocytes did not

vary significantly. Experiments involving the implantation of nude mice demonstrated that IDO⁺ keratinocytes lacked tumorigenicity. Importantly, IDO-overexpressed keratinocytes successfully constructed low-immunogenic epidermal cell sheets, and mouse wound healing experiments confirmed that IDO⁺ epidermal cell sheets have more effective wound repair capabilities, possibly by reducing wound tissue infiltration of CD3⁺ T lymphocytes, the level of inflammation in wound tissue, and the enhancement of the generation of new capillary-like structures in wound tissue.

Several autologous or allogenic cell sheet-based techniques are now being used more often in tissue engineering and regenerative medicine [35]. Allografts are now used as a temporary solution for several sorts of skin abnormalities. Allografts are susceptible to immunological rejection [36,37], which is a disadvantage of their use. Allogenic skin grafting starts a cascade of immunological responses in the recipient, culminating in the demise of the graft. Recent investigations [38–40] imply that IDO may play a crucial role in local immunosuppression. In an effort to construct a non-rejectable skin replacement comprised of allo- or xenogeneic skin cells, researchers are examining whether IDO may operate as a local immunosuppressive factor to prevent allo- or xenogeneic skin cell engraftment. Immune cells, but not principally fibroblasts, keratinocytes, and endothelial cells, are vulnerable to decreased tryptophan levels in the conditioned medium, according to previous research [27]. Hence, based on these data, we postulate that IDO may serve as a local immunosuppressive factor that prevents allo- or xenogeneic engraftment in animal models. In this research,

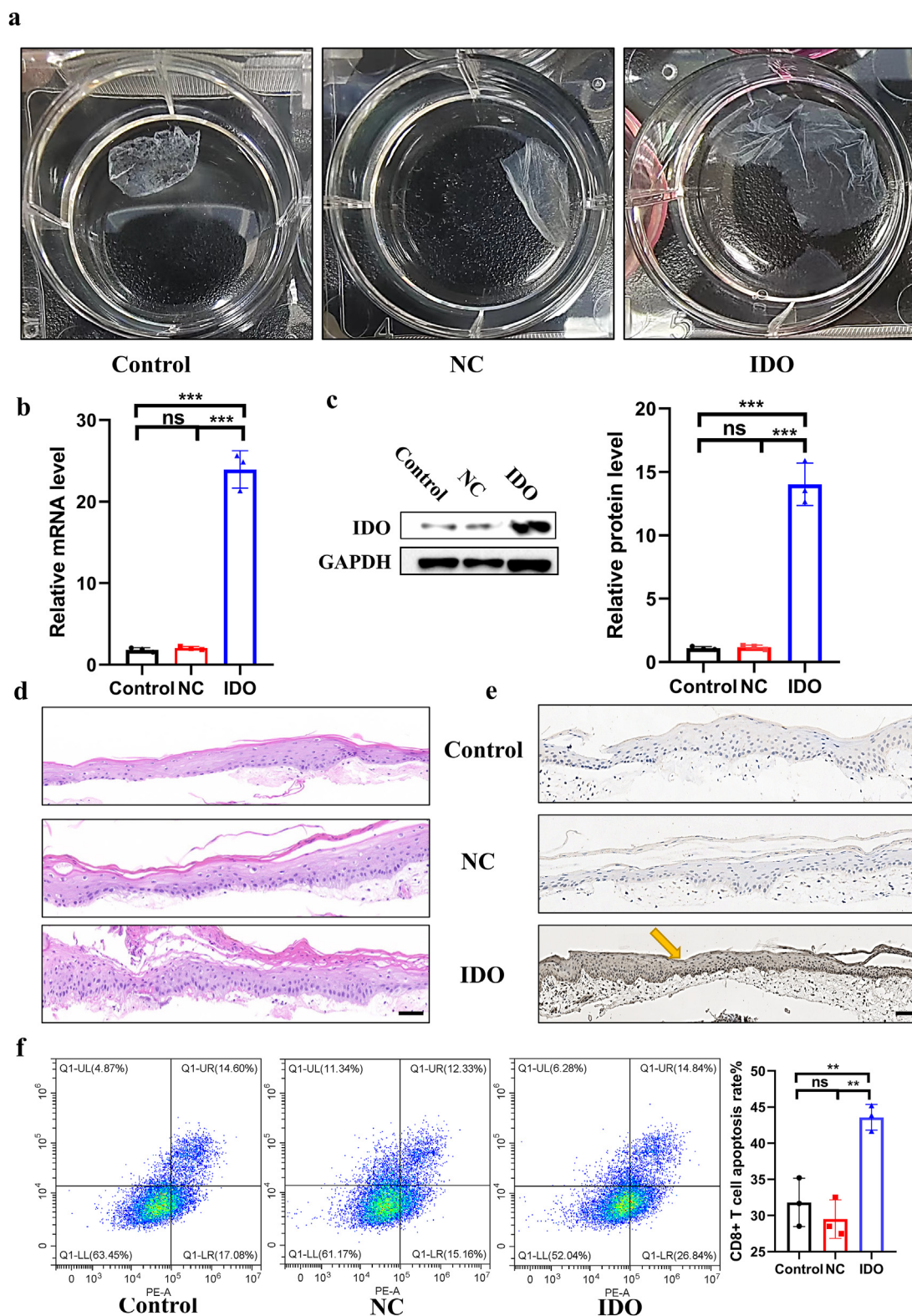


Fig. 3. Characteristics of IDO + keratinocyte cell sheets. **a.** Preparation of Epidermal Cell Sheets. (n = 5). **b.** Quantitative reverse transcription polymerase chain reaction was used to detect the IDO expression of cell sheets (**P < 0.01, ***P < 0.001, n = 3). **c.** Expression of IDO protein was evaluated in cell sheets by Western blot analysis (**P < 0.01, ***P < 0.001, n = 3). **d.** HE staining of cell sheets in the Control, NC and IDO group (Scale bar, 10 μm n = 5). **e.** IDO immunohistochemical staining of cell sheets in the Control, NC and IDO group. (Scale bar, 10 μm n = 5). **f.** Analysis of apoptosis of CD8⁺ T lymphocytes by flow cytometry (*P < 0.05, **P < 0.01, n = 3).

wounds treated with IDO + epidermal cell sheets healed quicker than those in the control and non-treated (NC) groups. At least two pathways may be responsible for the promotion of healing in wounds treated with IDO⁺ epidermal cell sheets, according to

further research. First, the logical explanation would be that the engrafted skin replacement stayed intact owing to IDO's protective function, resulting in quicker epithelialization and a shorter wound closure time. Another possible mechanism is the one shown in this

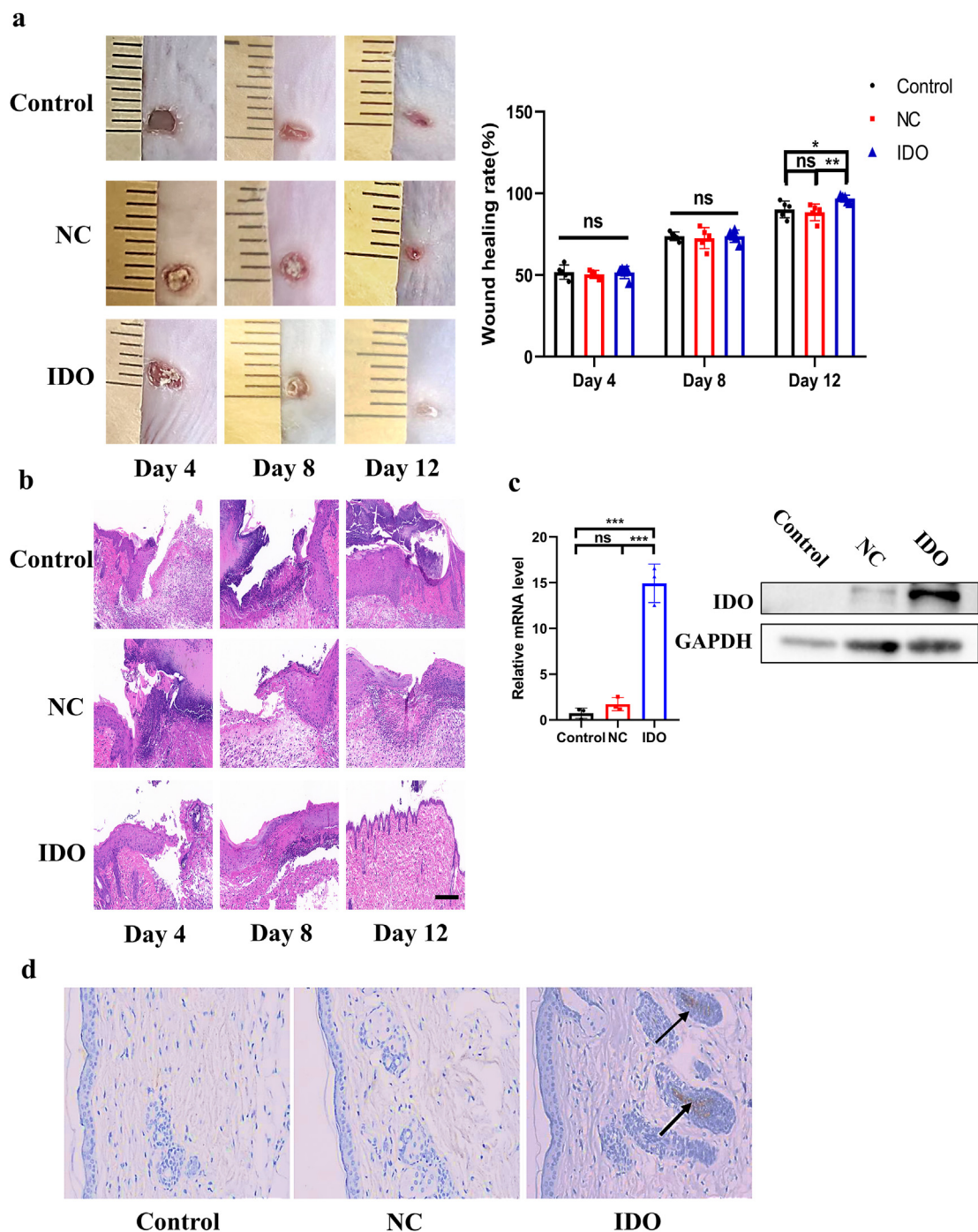


Fig. 4. IDO⁺ keratinocyte cell sheets promoting wound healing. **a.** Representative images showing wound healing on days 0, 4, 8 and 12 in Control, NC and IDO groups. Wound healing rates on days 4, 8 and 12 in Control, NC and IDO groups (**P* < 0.05 and ***P* < 0.01, *n* = 5). **b.** H&E staining of skin tissues in Control, NC and IDO groups on 4, 8 and 12 days, on day 12 after wounding, the epidermis in the IDO groups was closer to physiological conditions (Scale bar, 100 μm, *n* = 5). **c.** Expression of IDO mRNA and protein were evaluated in the Control, NC and IDO group by qPCR and Western blot analysis (****P* < 0.001, *n* = 3). **d.** Immunohistochemical staining for Human-specific IDO protein on day 12 wound tissue (*n* = 5).

research, namely that IDO stimulates angiogenesis, so promoting the healing process, at least in part. This discovery was further supported by the observation of a considerable reduction in the number of infiltrating CD3⁺ T cells after the transplantation of an IDO⁺ epidermal cell sheet. In addition, we discovered that IDO directly increases neovascularization in vivo, which may partially explain the accelerated recovery. Depletion of tryptophan by IDO in the immediate environment seems to contribute to the production

of capillary-like structures, primarily because the addition of tryptophan inhibits the formation of these structures by endothelial cells.

Delayed revascularization is one of the primary drawbacks of employing skin substitutes to cover wounds [41]. Young et al. [42] hypothesized that split-thickness skin grafts survive by diffusion of nutrients through the graft, early vascularization through inosculation, and eventually neovascularization. Composite skin

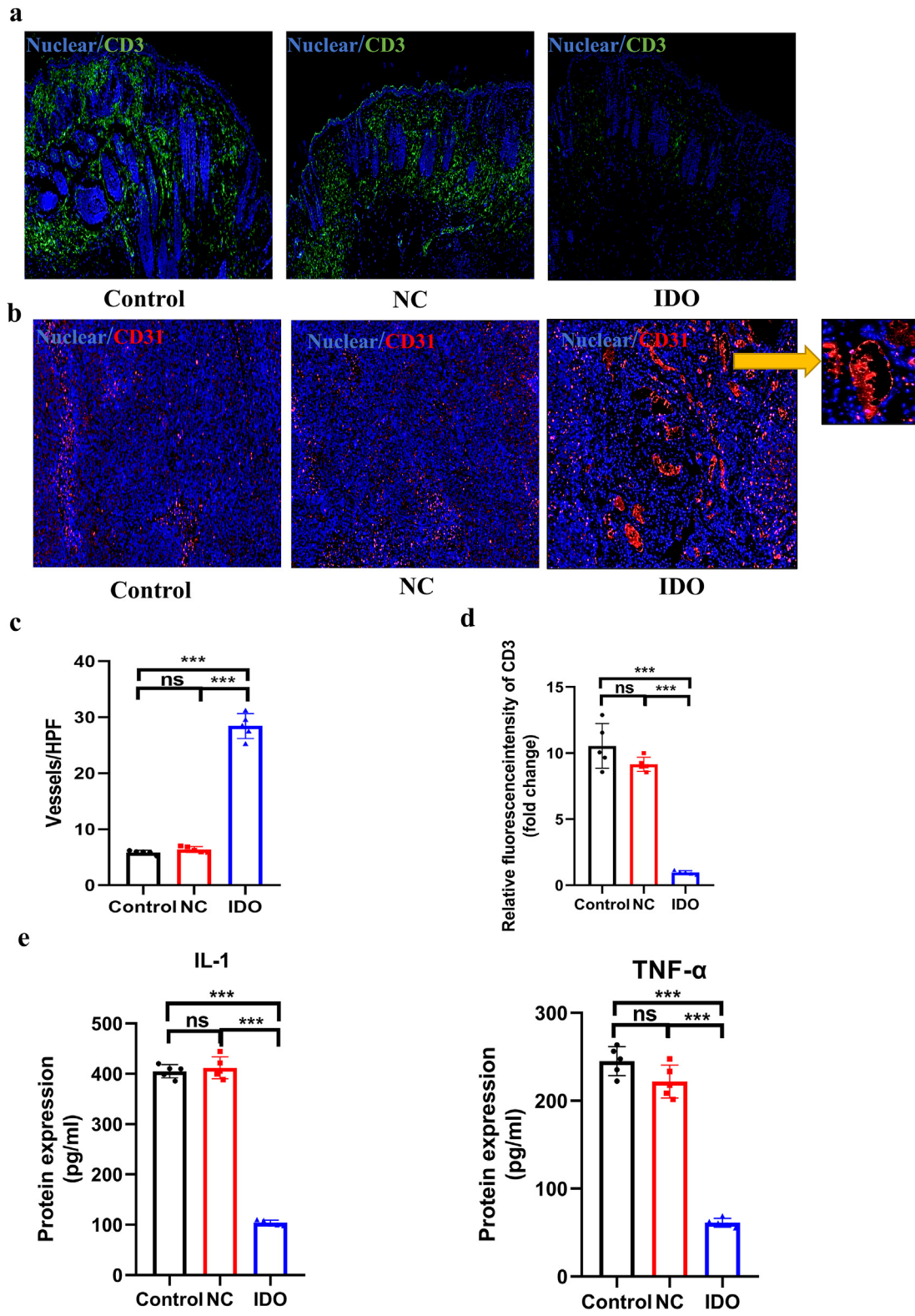


Fig. 5. Mechanism of IDO + epidermal cell sheet promoting wound healing. **a.** Immunofluorescence staining for CD3 on day 12 wound tissue (n = 5). **b.** Immunofluorescence staining for CD31 on day 12 wound tissue (n = 5). **c.** Quantitative analysis of capillary-like structures shown in (b) (**P < 0.01, n = 5). **d.** Quantitative analysis of CD3 T lymphocyte infiltration shown in (a) (**P < 0.01, n = 5). **e.** The expression of IL-1 and TNF- α in the grinding supernatant of wound tissue on the 12th day detected by ELISA (**P < 0.01, n = 5).

replacements cannot readily revascularize because they lack a capillary network. These grafts exclusively get nutrients through imbibition and neovascularization. Hence, unless neovascularization

is developed, imbibition alone is unlikely to be adequate to sustain the permanent implantation of skin replacements. The establishment of a capillary-like network in skin replacements by either

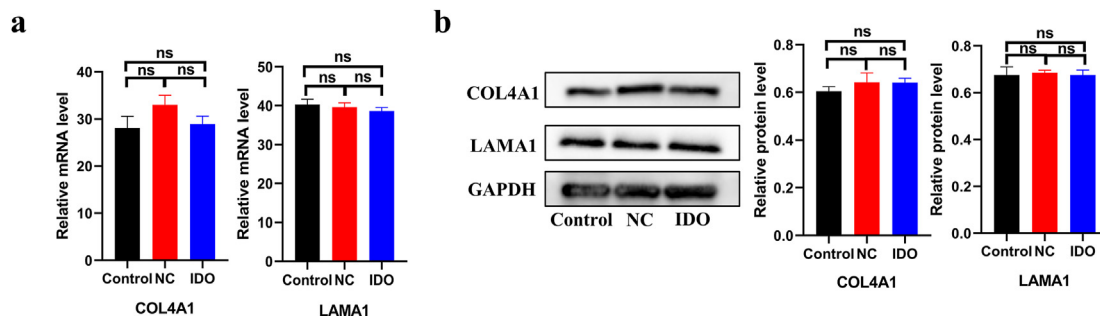


Fig. 6. **a.** Quantitative reverse transcription polymerase chain reaction was used to detect the gene expression of COL4A1 and LAMA1. (n = 3). **b.** Expression of COL4A1 and LAMA1 protein was evaluated in the Control, NC and IDO group by Western blot analysis (n = 3).

adding endothelial cells [43] or genetically altering skin cells with vascular endothelial growth factor [44] has been explored. These trials revealed that beginning neovascularization early considerably improves transplant acceptance. Fig. 5b demonstrates that in addition to preserving xenografted skin cells from immunological rejection, IDO seems to stimulate neovascularization in its earliest phases. Nonetheless, further research is necessary to comprehend how IDO induces angiogenesis in vivo and in vitro. Yet, our work may have limitations owing to possible variations between mouse and human skin. This may impede the complete extrapolation of clinical findings. This study did not verify the “survival time” of hypo-immunogenic cell sheets in the wounds of mice. However, in vitro data confirmed that low-immunogenic cell sheets can effectively promote apoptosis of CD8⁺ T lymphocytes and reduce immune protection and the inflammatory infiltration response. Therefore, in the future, we will use hypoimmunogenic cell sheets combined with functional hydrogels, 3D printing scaffolds and other polymer composites to develop more potential hypoimmunogenic materials. In addition, the creation of cell sheets takes around three weeks, which may restrict their practical applicability. Notwithstanding this, our research reveals the potential use of the low-immunogenic cell sheet in the treatment of skin wounds.

5. Conclusion

Our research concludes that our newly created hypoimmunogenic cell sheet may be useful in the treatment of skin excision wounds. Shown the viability of functional IDO-expressing skin allografts, which might address many of the problems associated with the scarcity of skin autografts without the necessity for immunosuppressive regimes that compromise immunological function.

Author contributions

H.Z. J.S and S.C. conceived and designed the experiments. W.T. contributed new reagents/analytic tools. J.B.wrote the manuscript. All authors analyzed and discussed the results and reviewed the manuscript. All authors have read and agreed to the published version of the manuscript.

Institutional review board statement

Human skin tissue samples were obtained from informed, consenting patients at the Fourth Medical Center of PLA General Hospital, This study was performed in compliance with the principles of the Helsinki Declaration and Guidelines for the Care and Use of Laboratory Animals of the Chinese Institute of Health. All procedures using animals were approved by the Animal Research

Committee and Ethics Committee of the General Hospital of PLA. We obtained written informed consent from all the patients who participated in this study.

Informed consent statement

Not applicable.

Data availability statement

The datasets used and/or analyzed during the current study are available from the corresponding author on reasonable request.

Funding information

This work was supported by the Science and Health joint project of Chongqing (2023MSXM073).

Declaration of competing interest

The authors have declared that no competing interest exists.

Acknowledgments

The authors would like to thank Peking University for providing CD8⁺T and HepG2 cells.

References

- [1] Zhang X, Kang X, Jin L, Bai J, Liu W, Wang Z. Stimulation of wound healing using bioinspired hydrogels with basic fibroblast growth factor (bFGF). *Int J Nanomed* 2018;13:3897–906. <https://doi.org/10.2147/IJN.S168998>.
- [2] Chang P, Li S, Sun Q, Guo K, Wang H, Li S, et al. Large full-thickness wounded skin regeneration using 3D-printed elastic scaffold with minimal functional unit of skin. *J Tissue Eng* 2022;13:20417314211063022. <https://doi.org/10.1177/20417314211063022>.
- [3] Zhang F, Zhang D, Cheng K, Zhou Z, Liu S, Chen L, et al. Spontaneous evolution of human skin fibroblasts into wound-healing keratinocyte-like cells. *Theranostics* 2019;9(18):5200–13. <https://doi.org/10.7150/tno.31526>.
- [4] Chen G, Qi Y, Niu L, Di T, Zhong J, Fang T, et al. Application of the cell sheet technique in tissue engineering. *Biomedical reports* 2015;3(6):749–57. <https://doi.org/10.3892/br.2015.522>.
- [5] Matsuura K, Utoh R, Nagase K, Okano T. Cell sheet approach for tissue engineering and regenerative medicine. *J Contr Release* 2014;190:228–39. <https://doi.org/10.1016/j.jconrel.2014.05.024>.
- [6] Zhao W, Chen H, Zhang Y, Zhou D, Liang L, Liu B, et al. Adaptive multi-degree-of-freedom in situ bioprinting robot for hair-follicle-inclusive skin repair: a preliminary study conducted in mice. *Bioeng Transl Med* 2022;7(3):e10303. <https://doi.org/10.1002/btm2.10303>.
- [7] Siemionow M, Strojny MM, Kozłowska K, Brodowska S, Grau-Kazmierczak W, Cwykiel J. Application of human epineural conduit supported with human mesenchymal stem cells as a novel therapy for enhancement of nerve gap regeneration. *Stem Cell Rev Rep* 2022;18(2):642–59. <https://doi.org/10.1007/s12015-021-10301-z>.

- [8] Dürr S, Kindler V. Implication of indoleamine 2,3 dioxygenase in the tolerance toward fetuses, tumors, and allografts. *J Leukoc Biol* 2013;93(5):681–7. <https://doi.org/10.1189/jlb.0712347>.
- [9] Chen WIDO. More than an enzyme. *Nat Immunol* 2011;12(9):809–11. <https://doi.org/10.1038/ni.2088>. Published 2011 Aug 18.
- [10] Munn DH, Zhou M, Attwood JT, Bondarev I, Conway SJ, Marshall B, et al. Prevention of allogeneic fetal rejection by tryptophan catabolism. *Science* 1998;281(5380):1191–3. <https://doi.org/10.1126/science.281.5380.1191>.
- [11] Munn DH, Sharma MD, Baban B, Harding HP, Zhang Y, Ron D, et al. GCN2 kinase in T cells mediates proliferative arrest and anergy induction in response to indoleamine 2,3-dioxygenase. *Immunity* 2005;22(5):633–42. <https://doi.org/10.1016/j.immuni.2005.03.013>.
- [12] Fallarino F, Grohmann U, You S, McGrath BC, Cavener DR, Vacca C, et al. The combined effects of tryptophan starvation and tryptophan catabolites down-regulate T cell receptor zeta-chain and induce a regulatory phenotype in naive T cells. *J Immunol* 2006;176(11):6752–61. <https://doi.org/10.4049/jimmunol.176.11.6752>.
- [13] Jalili RB, Forouzandeh F, Rezakhanlou AM, Hartwell R, Medina A, Warnock GL, et al. Local expression of indoleamine 2,3 dioxygenase in syngeneic fibroblasts significantly prolongs survival of an engineered three-dimensional islet allograft. *Diabetes* 2010;59(9):2219–27. <https://doi.org/10.2337/db09-1560>.
- [14] Takikawa O, Kuroiwa T, Yamazaki F, Kido R. Mechanism of interferon-gamma action. Characterization of indoleamine 2,3-dioxygenase in cultured human cells induced by interferon-gamma and evaluation of the enzyme-mediated tryptophan degradation in its anticellular activity. *J Biol Chem* 1988;263(4):2041–8.
- [15] Mazarei G, Budac DP, Lu G, Adomat H, Tomlinson Guns ES, Möller T, et al. Age-dependent alterations of the kynurenine pathway in the YAC128 mouse model of Huntington disease. *J Neurochem* 2013;127(6):852–67. <https://doi.org/10.1111/jnc.12350>.
- [16] Zhang B, Sun P, Shen C, Liu X, Sun J, Li D, et al. Role and mechanism of PI3K/AKT/FoxO1/PDX-1 signaling pathway in functional changes of pancreatic islets in rats after severe burns. *Life Sci* 2020 Oct 1;258:118145. <https://doi.org/10.1016/j.lfs.2020.118145>.
- [17] Liu Q-W, Liu Q-Y, Li J-Y, Wei L, Ren K-K, Zhang X-C, et al. Therapeutic efficiency of human amniotic epithelial stem cell-derived functional hepatocyte-like cells in mice with acute hepatic failure. *Stem Cell Res Ther* 2018 Nov 21;9(11):321. <https://doi.org/10.1186/s13287-018-1063-2>.
- [18] Wu M, Ji S, Xiao S, Kong Z, Fang H, Zhang Y, et al. JAM-A promotes wound healing by enhancing both homing and secretory activities of mesenchymal stem cells. *Clin Sci* 2015;129(7):575–88. <https://doi.org/10.1042/CS20140735>.
- [19] Miyawaki S, Kawamura Y, Oiwa Y, Shimizu A, Hachiya T, Bono H, et al. Tumour resistance in induced pluripotent stem cells derived from naked mole-rats. *Nat Commun* 2016;7:11471. <https://doi.org/10.1038/ncomms11471>.
- [20] Zhang F, Wang L, Wang JJ, Luo PF, Wang XT, Xia ZF. The caspase-1 inhibitor AC-VYAD-CMK attenuates acute gastric injury in mice: involvement of silencing NLRP3 inflammasome activities. *Sci Rep* 2016 Apr 7;6:24166. <https://doi.org/10.1038/srep24166>. PMID: 27053298; PMCID: PMC4823746.
- [21] Takikawa O, Kuroiwa T, Yamazaki F, Kido R. Mechanism of interferon-gamma action. Characterization of indoleamine 2,3-dioxygenase in cultured human cells induced by interferon-gamma and evaluation of the enzyme-mediated tryptophan degradation in its anticellular activity. *J Biol Chem* 1988 Feb 5;263(4):2041–8.
- [22] Li M, Ma J, Gao Y, Dong M, Zheng Z, Li Y, et al. Epithelial differentiation of human adipose-derived stem cells (hASCs) undergoing three-dimensional (3D) cultivation with collagen sponge scaffold (CSS) via an indirect co-culture strategy. *Stem Cell Res Ther* 2020 Mar 31;11(1):141. <https://doi.org/10.1186/s13287-020-01645-3>.
- [23] Sui Q, Liu D, Jiang W, Tang T, Kong L, Han K, et al. Dickkopf 1 impairs the tumor response to PD-1 blockade by inactivating CD8+ T cells in deficient mismatch repair colorectal cancer. *J Immunother Cancer* 2021;9(3). <https://doi.org/10.1136/jitc-2020-001498>.
- [24] Jia S, Guo P, Ge X, Wu H, Lu J, Fan X. Overexpression of indoleamine 2, 3-dioxygenase contributes to the repair of human airway epithelial cells inhibited by dexamethasone via affecting the MAPK/ERK signaling pathway. *Exp Ther Med* 2018 Jul;16(1):282–90. <https://doi.org/10.3892/etm.2018.6163>.
- [25] Liu QW, Liu QY, Li JY, Wei L, Ren KK, Zhang XC, et al. Therapeutic efficiency of human amniotic epithelial stem cell-derived functional hepatocyte-like cells in mice with acute hepatic failure. *Stem Cell Res Ther* 2018;21(1):321. <https://doi.org/10.1186/s13287-018-1063-2>.
- [26] Li M, Ma J, Gao Y, Dong M, Zheng Z, Li Y, et al. Epithelial differentiation of human adipose-derived stem cells (hASCs) undergoing three-dimensional (3D) cultivation with collagen sponge scaffold (CSS) via an indirect co-culture strategy. *Stem Cell Res Ther* 2020;31(1):141. <https://doi.org/10.1186/s13287-020-01645-3>.
- [27] Ghahary A, Li Y, Tredget EE, Kilani RT, Iwashina T, Karami A, et al. Expression of indoleamine 2,3-dioxygenase in dermal fibroblasts functions as a local immunosuppressive factor. *J Invest Dermatol* 2004 Apr;122(4):953–64. <https://doi.org/10.1111/j.0022-202X.2004.22409.x>.
- [28] Sher SE, Hull BE, Rosen S, Church D, Friedman L, Bell E. Acceptance of allogeneic fibroblasts in skin equivalent transplants. *Transplantation* 1983 Nov;36(5):552–7. <https://doi.org/10.1097/00007890-198311000-00015>.
- [29] Hultman CS, Brinson GM, Siltharm S, deSerres S, Cairns BA, Peterson HD, et al. Allogeneic fibroblasts used to grow cultured epidermal autografts persist in vivo and sensitize the graft recipient for accelerated second-set rejection. *J Trauma* 1996 Jul;41(1):51–8. <https://doi.org/10.1097/00005373-199607000-00009>. ; discussion 58–60.
- [30] Erdag G, Morgan JR. Allogeneic versus xenogeneic immune reaction to bio-engineered skin grafts. *Cell Transplant* 2004;13(6):701–12. <https://doi.org/10.3727/000000004783983594>.
- [31] Schmidt P, Krook H, Maeda A, Korsgren O, Benda B. A new murine model of islet xenograft rejection: graft destruction is dependent on a major histocompatibility-specific interaction between T-cells and macrophages. *Diabetes* 2003 May;52(5):1111–8. <https://doi.org/10.2337/diabetes.52.5.1111>.
- [32] Şik S, Er E, Soysal Y, İmirzalioglu N. Prolongation of skin xenograft survival with modified cultured fibroblasts. *Plast Reconstr Surg* 2003 Jan;111(1):275–82. <https://doi.org/10.1097/01.PRS.0000034939.51369.5B>. ; discussion 283–5.
- [33] Schwenker F, Schneider BL, Pralong WF, Déglon N, Aebischer P. Survival of encapsulated human primary fibroblasts and erythropoietin expression under xenogeneic conditions. *Hum Gene Ther* 2004 Jul;15(7):669–80. <https://doi.org/10.1089/1043034041361172>. PMID: 15242527.
- [34] Boyce ST, Supp AP, Harriger MD, Greenhalgh DG, Warden GD. Topical nutrients promote engraftment and inhibit wound contraction of cultured skin substitutes in athymic mice. *J Invest Dermatol* 1995 Mar;104(3):345–9. <https://doi.org/10.1111/1523-1747.ep12665374>.
- [35] Matsuura K, Utoh R, Nagase K, Okano T. Cell sheet approach for tissue engineering and regenerative medicine. *J Contr Release* 2014 Sep 28;190:228–39. <https://doi.org/10.1016/j.jconrel.2014.05.024>. Epub 2014 May 21.
- [36] Roh JL, Jang H, Lee J, Kim EH, Shin D. Promotion of oral surgical wound healing using autologous mucosal cell sheets. *Oral Oncol* 2017 Jun;69:84–91. <https://doi.org/10.1016/j.oraloncology.2017.04.012>.
- [37] Aydogmus U, Topkara A, Akbulut M, Ozkan A, Turk F, Sahin B, et al. Effectiveness of palatal mucosa graft in surgical treatment of sub-glottic stenosis. *Clin Exp Otorhinolaryngol* 2016 Dec;9(4):358–65. <https://doi.org/10.21053/ceo.2015.01508>.
- [38] Munn DH, Zhou M, Attwood JT, Bondarev I, Conway SJ, Marshall B, et al. Prevention of allogeneic fetal rejection by tryptophan catabolism. *Science* 1998 Aug 21;281(5380):1191–3. <https://doi.org/10.1126/science.281.5380.1191>.
- [39] Frumento G, Rotondo R, Tonetti M, Damonte G, Benatti U, Ferrara GB. Tryptophan-derived catabolites are responsible for inhibition of T and natural killer cell proliferation induced by indoleamine 2,3-dioxygenase. *J Exp Med* 2002 Aug 19;196(4):459–68. <https://doi.org/10.1084/jem.20020121>.
- [40] Uyttenhove C, Pilotte L, Théate I, Stroobant V, Colau D, Parmentier N, et al. Evidence for a tumoral immune resistance mechanism based on tryptophan degradation by indoleamine 2,3-dioxygenase. *Nat Med* 2003 Oct;9(10):1269–74. <https://doi.org/10.1038/nm934>.
- [41] Sahota PS, Burn JL, Brown NJ, MacNeil S. Approaches to improve angiogenesis in tissue-engineered skin. *Wound Repair Regen* 2004 Nov-Dec;12(6):635–42. <https://doi.org/10.1111/j.1067-1927.2004.12608.x>.
- [42] Young DM, Greulich KM, Weier HG. Species-specific in situ hybridization with fluorochrome-labeled DNA probes to study vascularization of human skin grafts on athymic mice. *J Burn Care Rehabil* 1996 Jul-Aug;17(4):305–10. <https://doi.org/10.1097/00004630-199607000-00005>.
- [43] Black AF, Berthod F, L'heureux N, Germain L, Auger FA. In vitro reconstruction of a human capillary-like network in a tissue-engineered skin equivalent. *Faseb J* 1998 Oct;12(13):1331–40. <https://doi.org/10.1096/fasebj.12.13.1331>.
- [44] Supp DM, Supp AP, Bell SM, Boyce ST. Enhanced vascularization of cultured skin substitutes genetically modified to overexpress vascular endothelial growth factor. *J Invest Dermatol* 2000 Jan;114(1):5–13. <https://doi.org/10.1046/j.1523-1747.2000.00824.x>.